



**HAL**  
open science

## Dynamics of a three-phase upflow fixed bed catalytic reactor

Carine Julcour-Lebigue, Franck Stüber, Jean-Marc Le Lann, Anne-Marie Wilhelm, Henri Delmas

► **To cite this version:**

Carine Julcour-Lebigue, Franck Stüber, Jean-Marc Le Lann, Anne-Marie Wilhelm, Henri Delmas. Dynamics of a three-phase upflow fixed bed catalytic reactor. *Chemical Engineering Science*, 1999, vol. 54, pp. 2391-2400. 10.1016/S0009-2509(98)00304-2. hal-00731121

**HAL Id: hal-00731121**

**<https://hal.science/hal-00731121>**

Submitted on 12 Sep 2012

**HAL** is a multi-disciplinary open access archive for the deposit and dissemination of scientific research documents, whether they are published or not. The documents may come from teaching and research institutions in France or abroad, or from public or private research centers.

L'archive ouverte pluridisciplinaire **HAL**, est destinée au dépôt et à la diffusion de documents scientifiques de niveau recherche, publiés ou non, émanant des établissements d'enseignement et de recherche français ou étrangers, des laboratoires publics ou privés.

# Dynamics of a three-phase upflow fixed bed catalytic reactor

C. Julcour, F. Stüber, J. M. Le Lann, A. M. Wilhelm, H. Delmas\*

Laboratoire de Génie Chimique, CNRS ENSIGC/INPT, 18 Chemin de la Loge,  
31078 Toulouse Cedex, France

\* Corresponding author

## Abstract

A dynamic model of an upflow fixed bed catalytic reactor is developed to examine numerically transient axial temperature and concentration profiles obtained for the consecutive hydrogenation of 1,5,9-cyclododecatriene on a Pd/Al<sub>2</sub>O<sub>3</sub> catalyst.

This non-isothermal heterogeneous model includes the resistances to heat and mass transfer at the gas-liquid and liquid-solid interfaces, as well as the heat exchanges through the jacket of the reactor.

The predictions of the model are compared to experimental data for various gas and liquid flow rates to describe dynamic events, such as the start-up of the reactor and the effects of sudden changes in the operating conditions on the reactor behavior and its thermal stability. The predicted transient profiles are in good agreement with the experimental measurements. Still, the dynamic model is not able to correctly predict hot spots and runaways experimentally observed at very high hydrogen flow rates.

*Keywords:* fixed bed reactor; cocurrent upflow; dynamic modeling

## INTRODUCTION

Reactor control and reactor safety are important features in the design and operation of industrial processes that carry out complex reactions with constraints of thermal stability or/and selectivity as for example exothermic hydrogenation reactions. In this light, a dynamic model of the reactor is very useful to study both the start-up period and the effects of a sudden (accidental) change in the operating conditions, particularly on the thermal reactor stability. So far steady state models of multiphase fixed bed reactors have been extensively developed in several reviews (Herskowitz and Smith, 1983; Zhukova *et al.*, 1990; Gianetto and Specchia, 1992), while only a few papers have investigated their transient behavior.

Feick *et al.* (1970), Visser *et al.* (1994) compared models of various complexities to describe the dynamic behavior of packed bed reactors. Wärna *et al.* (1996) performed dynamic models for slurry and fixed bed reactors operating in non-isothermal conditions. The dynamic model of the fixed bed reactor was applied to describe the start-up of a fixed bed reactor during the hydrogenation of toluene on a Ni/Al<sub>2</sub>O<sub>3</sub> catalyst.

These studies put clearly in evidence the relevance of a dynamic model and the lack of comparison between the model predictions and transient experimental data.

The objective of this work is to examine numerically the transient concentration and temperature profiles obtained in a cocurrent upflow fixed bed reactor during the consecutive hydrogenation of 1,5,9-cyclododecatriene (CDT) on a 0.5% Pd/Al<sub>2</sub>O<sub>3</sub> shell catalyst. For that purpose an existing steady state model of the reactor (Stüber *et al.*, 1996) has been extended to develop a dynamic model. Transient responses of the system respective to a change in flow

rates as well as thermal reactor stability are investigated and fully described. Simulations with various flow rates of gas and liquid are performed and compared with experimental results obtained with the pilot upflow reactor.

## EXPERIMENTAL

The experimental apparatus is shown in Fig. 1. The reactor unit consists of a jacketed packed bed tube with an inner diameter of 0.026 m and a bed height of 1.5 m. The tube is filled with cylindrical alumina pellets of 3.1 mm diameter coated with palladium to a depth of 250  $\mu\text{m}$  (Degussa, E263/D, 0.5% Pd). A flexible grid is located at the top of the reactor to prevent particle fluidization during operation.

Five temperature probes as well as five liquid sample valves are located along the reactor in order to measure axial temperature and concentration profiles. One of these probes is made of three thermocouples of type K, radially distanced, in order to check for radial temperature gradients. The other probes are of type Pt100. Temperatures are monitored using a data acquisition system implemented on a microcomputer. Temperature control in the reactor is achieved by means of cooling oil circulating in the jacket at a nearly constant temperature (423 K).

Liquid samples are rapidly withdrawn to obtain an axial profile within less than two minutes. The samples are analyzed by a HP 5890 gas chromatograph equipped with a HP-FFAP capillary column.

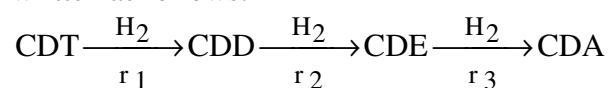
Before entering the reactor, the gas and liquid phases are mixed in an inert fixed bed in order to homogenize the temperature of the two phases and achieve gas-liquid equilibrium.

In order to prevent the reaction to start before the beginning of the experiment, the following procedure for the start-up of the reactor has proved to be convenient. The reactor is fed with cyclododecatriene and pre-heated to 70°C. Then the thermal oil is bypassed in an outer circuit and heated up to 200°C.

Once the oil has reached the required temperature, the hydrogen flow inlet valve is opened to build up within a few seconds the operating pressure in the reactor. Then the oil is allowed to circulate again in the double jacket, which corresponds to the initial time of the experiment. The oil temperature stabilizes rapidly at a constant temperature of 150°C and thus, only the dynamics of the three-phase reaction has to be accounted for in the modeling.

Experimental runs are performed at a pressure of 0.4 MPa and at high temperatures (above 433 K). Liquid flow rate varies from 0.55 l/h to 1.9 l/h, and gas flow rate from 125 NI/h up to 790 NI/h for normal working conditions and up to 1350 NI/h to cause a hot spot in the reactor.

The products of the reaction are consecutively: cyclododecadiene (CDD), cyclododecene (CDE) and cyclododecane (CDA). A simplified reaction scheme lumping isomers may be written as follows:



## DYNAMIC MODELING OF THE THREE-PHASE CATALYTIC UPFLOW REACTOR

A non-isothermal heterogeneous model is chosen to account for both mass and heat transfer limitations at the gas-liquid and liquid-solid interfaces and the heat exchanges through the reactor walls, including the thermal balance of the cooling fluid.

Unlike the previously studied steady state model (Stüber *et al.*, 1996), it introduces separate mass and heat balances for the gas phase. The calculation of the liquid holdup and the phase enthalpies has also been included. Because of the introduction of the dynamics, a different numerical treatment has been used.

### FUNDAMENTAL ASSUMPTIONS

The dynamic model of the fixed bed reactor is based on the following assumptions:

1. The radial gradients are negligible: the ratio of reactor diameter (0.026 m) to reactor length (1.5 m) is indeed very small, and this hypothesis has been confirmed by radial temperature measurements. Thus we use a one-space dimension model.
2. The vaporization of the organic components is not considered due to their very low vapor pressures: the gas phase is pure hydrogen, and the overall molar flow rate of liquid is supposed to be constant, as the solubility of hydrogen is very low.
3. Since the measurements do not permit to distinguish between gas and liquid phase temperatures, an arbitrarily high gas-liquid heat transfer coefficient is used to describe the heat exchange between the two phases, leading to nearly the same temperature in both phases. Heat transfer with the inner reactor wall is assumed to occur through the liquid phase only. The outer reactor wall is supposed to be perfectly insulated.
4. Since the concentration of CDT is very high compared to hydrogen solubility, the diffusion limitations of organic components inside the catalyst particle are assumed to be negligible and the pellet is a gradientless volume for the organics. However as the hydrogen diffusion in the pores has been proved to be very limiting, no accumulation of hydrogen in the catalyst phase is considered. In order to take into account the hydrogen diffusion limitation in the reaction term, an apparent kinetic law is used to describe the consecutive hydrogenation (Stüber, 1995):

$$R_{i,\text{app}} = \frac{k_i K_j C_j C_{\text{H}_2}^{\alpha_i}}{1 + \sum_{j=1}^3 K_j C_j} \quad (\alpha_1 = \alpha_2 = 1, \alpha_3 = 1.32)$$

where  $i$  is the reaction number, and  $j$  is the component number ( $j = 1$ : CDT,  $2$ : CDD,  $3$ : CDE).

The Arrhenius law defines the rate constants  $k_i$  and adsorption constants  $K_j$ :

$$k_i = k_{i,0} \exp(-E_i/RT) \quad \text{and} \quad K_j = K_{j,0} \exp(-A_j/RT).$$

Moreover the catalyst pellet is supposed to be isothermal.

5. Plug flow is assumed for the gas phase, but liquid axial dispersion effects are taken into account.

## EQUATIONS OF THE MODEL

Based on the assumptions described before, the dynamic model is given by the following set of equations:

### Mass balances

*Liquid phase* (plug flow with axial dispersion)

$$\frac{\partial}{\partial t}(\varepsilon_L C_{L,i}) = \frac{\partial}{\partial z} \left( \varepsilon_L D_{zL} \frac{\partial C_{L,i}}{\partial z} \right) - \frac{\partial F_{L,i}}{\partial z} + (N_{GL,i} - N_{LS,i}) \quad (1)$$

$i = \text{CDT, CDD, CDE, CDA, H}_2$

with  $N_{GL,k} = 0$   $k = \text{CDT, CDD, CDE, CDA}$  as only hydrogen is present in the gas phase

$$N_{GL,H_2} = k_L a (C_{L,H_2}^* - C_{L,H_2})$$

$$\text{and } N_{LS,i} = (k_S a_S)_i (C_{L,i} - C_{S,i})$$

*Catalyst phase*

Assumptions in point 4 lead to the following equations for the catalyst phase:

$$\varepsilon_p (1 - \varepsilon_{bv}) \frac{\partial}{\partial t} (C_{S,k}) = (N_{LS,k} - \rho_B R_{S,k}) \quad k = \text{CDT, CDD, CDE, CDA} \quad (2)$$

$$0 = N_{LS,H_2} - \rho_B R_{S,H_2}$$

where  $R_{S,\text{CDT}} = R_{1,\text{app}}(C_{S,i}, T_S)$

$$R_{S,\text{CDD}} = R_{2,\text{app}}(C_{S,i}, T_S) - R_{1,\text{app}}(C_{S,i}, T_S)$$

$$R_{S,\text{CDE}} = R_{3,\text{app}}(C_{S,i}, T_S) - R_{2,\text{app}}(C_{S,i}, T_S)$$

$$R_{S,\text{CDA}} = -R_{3,\text{app}}(C_{S,i}, T_S)$$

$$R_{S,H_2} = R_{1,\text{app}}(C_{S,i}, T_S) + R_{2,\text{app}}(C_{S,i}, T_S) + R_{3,\text{app}}(C_{S,i}, T_S)$$

*Gas phase* (plug flow)

$$\frac{\partial}{\partial t}(\varepsilon_G C_{G,H_2}) = -\frac{\partial F_{G,H_2}}{\partial z} - N_{GL,H_2} \quad (3)$$

### Energy balances

The heat exchanges through the walls of the reactor are represented in Fig. 2.

Enthalpy models are described in separate equations to present a general form of the model.

*Liquid phase*

$$\frac{\partial}{\partial t}(\varepsilon_L H_L) = \frac{\partial}{\partial z} \left( \Lambda_{zL} \frac{\partial T_L}{\partial z} \right) - \frac{\partial}{\partial z} \left( \sum_i (F_{L,i} H'_{L,i}) \right) + (h_{LS} a_S)(T_S - T_L)$$

$$- \frac{h_1 A_1}{V_R} (T_L - T_{W1}) + (h_{LG} a)(T_G - T_L) \quad (4)$$

*Catalyst phase*

$$\frac{\partial H_S}{\partial t} = -(h_{LS}a_S)(T_S - T_L) - (R_{S,H2}\Delta H_R\rho_B) \quad (5)$$

*Gas phase (hydrogen only)*

$$\frac{\partial}{\partial t}(\varepsilon_G H_G) = -\frac{\partial}{\partial z}(F_{G,H2}H'_G) - (h_{GL}a)(T_G - T_L) \quad (6)$$

*Cooling oil (Marlotherm)*

$$\frac{\partial H_M}{\partial t} = -\frac{\partial}{\partial z}(F_M H'_M) + \frac{h_2 A_1}{V_{an}}(T_{W1} - T_M) - \frac{h_3 A_2}{V_{an}}(T_M - T_{W2}) \quad (7)$$

*Wall 1*

$$V_{W1}\rho_{st}C'_{P,st}\frac{\partial T_{W1}}{\partial t} = h_1 A_1(T_L - T_{W1}) - h_2 A_1(T_{W1} - T_M) \quad (8)$$

*Wall 2*

As the external reactor wall is assumed to be perfectly insulated:

$$V_{W2}\rho_{st}C'_{P,st}\frac{\partial T_{W2}}{\partial t} = h_3 A_2(T_M - T_{W2}) \quad (9)$$

Pressure drop

$$\frac{\partial P}{\partial z} + f_{GL} \times 2 \frac{u_G^2 \rho_G}{d_{eq}} + \varepsilon_L \rho_L g = 0 \quad (10)$$

Description of liquid holdup and enthalpies

$$\varepsilon_L - m\varepsilon_L = 0 \quad \text{with } m\varepsilon_L \text{ the model for the liquid holdup} \quad (11)$$

$$H_L - mH_L = 0 \quad mH_L = \sum_i C_{L,i} \int_{T_{ref}}^{T_L} C_{P,Li}(T) dT \quad (12)$$

$$H_S - mH_S = 0 \quad (13)$$

For the catalyst phase enthalpy calculation, both the enthalpy of the solid and the enthalpy of the liquid contained in the pores of the pellet are considered:

$$mH_S = (1 - \varepsilon_{bv}) \int_{T_{ref}}^{T_S} (\rho_{Ap} C'_{P,p}(T) + \varepsilon_p \rho_{Lp} C'_{P,Lp}(T)) dT$$

$$H_G - mH_G = 0 \quad mH_G = C_{G,H2} \int_{T_{ref}}^{T_G} C_{P,GH2}(T) dT \quad (14)$$

$$H_M - mH_M = 0 \quad mH_M = \int_{T_{ref}}^{T_M} \rho_M C'_{P,M}(T) dT \quad (15)$$

$$C_{G,H2} - \frac{\rho_{G,H2}}{M_{H2}} = 0 \quad (16)$$

## Initial and boundary conditions

### *Boundary conditions*

For the liquid phase, Danckwerts' conditions are used:

at  $z = 0$  and  $\forall t$

$$\varepsilon_L D_{zL} \frac{\partial C_{L,i}}{\partial z} = (F_{L,i})_{z=0} - (F_{L,i})_{\text{inlet}} \quad i = \text{CDT, CDD, CDE, CDA, H}_2 \quad (17)$$

$$\left( \frac{\Lambda_{zL}}{\rho_L C'_{P,L} u_L} \right) \frac{\partial T_L}{\partial z} = (T_L)_{z=0} - (T_L)_{\text{inlet}} \quad (18)$$

at  $z = L_R$  and  $\forall t$

$$\frac{\partial C_{L,i}}{\partial z} = 0 \quad (19)$$

$$\frac{\partial T_L}{\partial z} = 0 \quad (20)$$

### *Initial conditions*

The liquid phase contains CDT saturated with  $\text{H}_2$ . The concentrations in the catalyst phase equal the concentrations in the liquid phase.

The hydrogen flow rate is uniform along the reactor.

The temperatures of the gas, liquid and catalyst phases are all equal to the inlet temperature of the gas-liquid mixture.

The set of partial differential and algebraic equations (PDAE) is reduced by the method of lines: spatial derivatives are discretized and the resultant DAE system is solved by the software package RESEDA (Le Lann, 1996), using the Gear method (Hindmarsh, 1980).

## **MODEL PARAMETERS**

For the calculation of the liquid holdup  $\varepsilon_L$ , the gas-liquid mass transfer coefficient  $k_{L,a}$ , the liquid-solid mass transfer coefficient of hydrogen  $(k_{S,aS})_{\text{H}_2}$ , and the wall heat transfer coefficient  $h_1$ , empirical correlations have been established using the same reaction and reactor system (Stüber, 1995): they depend above all on the gas flow rate.

The correlations of Specchia *et al.* (1978), Turpin and Huntington (1967) and Syaiful (1992) are used respectively for the solid-liquid mass transfer coefficients of the organic components, the pressure drop and the axial dispersion coefficient calculations.

The axial conductivity is deduced from the analogy of mass and heat transfer:  $Pe_L = Pe_T$ .

Except for the lowest flow rates, the liquid dispersion (both for mass and heat) was found to be negligible.

For the gas-liquid heat transfer, a high coefficient has been used, based on the assumption that the temperatures of both gas and liquid phases are the same.

## **RESULTS AND DISCUSSION**

### **PRELIMINARY SIMULATIONS**

The dynamic model was first assessed for the plug flow mode by comparing its predictions when steady state conditions are reached with the results of a steady state model where spatial derivatives are integrated by the Gear method.

From  $N$  equal to 10, the dynamic model was checked to give the same axial concentration profiles as the steady state model.

However in order to describe more precisely the axial temperature profile (which is relatively steep near the reactor inlet), 40 sub-divisions were used to discretize the reactor.

The numerical results underscore the influence of three parameters:

- Hydrogen gas-liquid and liquid-solid mass transfer coefficients for the axial concentration profiles.

- Wall heat transfer coefficient for the axial temperature profile.

The empirical parameter correlations had to be slightly corrected in order to fit the experimental data: the hydrogen gas-liquid and liquid-solid mass transfer coefficients were increased by 25 % and the wall heat transfer coefficient by 20 % for the low liquid flow rates. Moreover between two experimental measurement series a deactivation of the catalyst was observed and included in the dynamic model by means of a deactivation factor.

### *START-UP OF THE REACTOR*

The dynamic model was then tested to describe the effective and real start-up of the fixed bed reactor for various flow rate conditions. Transient axial temperature and concentration profiles were compared with the experimental values.

Fig. 3 and 4 show axial concentration profiles at different times before steady state conditions: the model predicts a minimum for the concentration of CDT, which was experimentally checked. This minimum moves towards the top of the reactor when time increases and disappears when steady state conditions are reached (cf. Fig. 5). It is due to the strong differences in the values of the gas and the liquid velocities and to the initial conditions (at  $t = 0$  the column is full of cyclododecatriene saturated with hydrogen at a low temperature). At 10 minutes, as the liquid front has reached the middle of the column (the residence time of the liquid is about 15 minutes), there is near the top of the reactor a zone of "initial" liquid that is still rich in cyclododecatriene. Indeed it has reacted with an impoverished hydrogen gas flow.

An example of time evolution of concentrations and temperature for a given axial position in the reactor is plotted in Fig. 6 and 7. As shown by these figures, the numerical results are in quite good agreement with the experimental data.

For the axial positions near the top of the reactor, the CDD concentration-time curve can exhibit a maximum (cf. Fig. 6), which tends to disappear when increasing liquid velocity. This maximum can even be obtained for the desired product CDE for the lowest liquid flow rate.

In the investigated range of operating conditions, constant outlet concentrations are reached within 20 minutes for a liquid flow rate of 1.9 l/h (corresponding to a residence time of about 10 minutes) and within more than 60 minutes for the lowest flow rate (0.55 l/h). Only 10 minutes are required to reach steady temperature profiles (cf. Fig. 7).

### *RESPONSE TO A CHANGE IN OPERATING CONDITIONS*

In order to investigate further the reliability of the dynamic model, it was used to predict the influence of a step change in the gas or liquid flow rate.

Increasing or decreasing flow rate steps up to 100 % were imposed to the reactor and the predicted time-concentration curves were compared to experimental responses.

Fig. 8 gives a typical response of the system to such a sudden increase in the liquid flow rate. It is seen that the reaction conversion decreases to reach the second steady state profile after a period of 15 minutes, representing nearly twice the estimated residence time after the step change.

The dynamic model was also able to predict the response of the time-temperature curve when increasing or decreasing the gas flow rate. However for the case of a step in the liquid flow rate the predicted temperature evolution was slightly distinct from the experimental one. This may be due to the correlation used for the calculation of the wall heat transfer coefficient.

#### *HOT SPOTS AND RUNAWAY*

Finally, the thermal stability of the reactor was studied by increasing the gas flow rate until a hot spot is detected. In Fig. 9, a hot spot appeared experimentally after a two-step increase of the gas flow rate.

The dynamic model was able to fit the first increase in temperature, but it predicts stabilization after the second step. This different behavior predicted by the dynamic model may be explained by the erroneous extrapolation of kinetics at higher temperature. But more probably the extrapolation of empirical hydrodynamic and transfer correlations at higher gas flow rate is no more possible, since the flow pattern of the bed should change, according to Stüber (1995) from pulse flow to spray flow. The lack of description of the dynamic phenomena at the catalyst pellet scale (in particular on assuming complete wetting of the catalyst) may also be a reason for the model failure.

Moreover the model doesn't take into account radial temperature gradients which may be non-negligible at high temperature.

#### **CONCLUSION**

A dynamic model of a three-phase fixed bed reactor was developed and tested with the consecutive hydrogenation of 1,5,9-cyclododecatriene on Pd/Al<sub>2</sub>O<sub>3</sub>. The model accounts for the limitations to heat and mass transfer at gas-liquid interface and catalyst surface, as well as the heat transport through the reactor jacket. It consists of partial differential and algebraic equations that were solved by the method of lines.

The dynamic modeling proved its reliability to describe the start-up of the reaction as well as the response to a gas or liquid flow rate variation at normal working conditions.

Still it is not able to correctly predict hot spots and needs improvements, in particular by including the description of the phenomena at the catalyst pellet scale (resistances to heat and mass transfer within the porous structure of the catalyst).

The results presented here show that a model with numerous parameters can be convenient to describe steady state conditions and responses to moderate disturbances, but not runaways. Such a model must be used with caution at the limits of the reactor stability where information has to be the most precise.

## NOTATION

$A_1$	= inner wall reactor surface (wall 1), $m^2$
$A_2$	= outer wall reactor surface (wall 2), $m^2$
$C$	= concentration, $mol/m^3$
$C_{L,H_2}^*$	= dissolved hydrogen concentration at the gas-liquid interface, $mol/m^3$
$C_P$	= specific heat, $J/mol/K$
$C'_P$	= specific heat, $J/kg/K$
$d_{eq}$	= equivalent particle diameter, $m$
$D_{zL}$	= axial dispersion coefficient, $m^2/s$
$F$	= molar flow rate per surface unit, $mol/m^2/s$
$f_{GL}$	= two-phase friction factor
$k_{La}$	= gas-liquid volumetric mass transfer coefficient, $1/s$
$k_{sAs}$	= liquid-solid mass transfer coefficient, $1/s$
$H$	= enthalpy per volume unit, $J/m^3$
$H'$	= molar enthalpy, $J/mol$
$h_1$	= bed to wall 1 heat transfer coefficient, $W/m^2/K$
$h_2$	= wall 1 to cooling oil heat transfer coefficient, $W/m^2/K$
$h_3$	= cooling oil to wall 2 heat transfer coefficient, $W/m^2/K$
$h_{GL}$	= gas to liquid heat transfer coefficient, $W/m^2/K$
$h_{LS}$	= liquid to solid heat transfer coefficient, $W/m^2/K$
$L_R$	= reactor length, $m$
$Pe_L$	= liquid phase mass Peclet number
$Pe_T$	= liquid phase thermal Peclet number
$R$	= reaction rate per catalyst weight, $mol/s/kg$
$T$	= temperature, $K$
$u$	= velocity, $m/s$
$V_{an}$	= annular volume, $m^3$
$V_{W1}$	= volume of wall 1, $m^3$
$V_{W2}$	= volume of wall 2, $m^3$
$V_R$	= reactor inner volume, $m^3$

### *Greek symbols*

$\epsilon$	= holdup
$\epsilon_{bv}$	= bed void fraction
$\epsilon_p$	= porosity of the catalyst pellet
$\rho$	= density, $kg/m^3$
$\rho_{Ap}$	= apparent density of the catalyst pellet, $kg/m^3$
$\rho_B$	= catalyst bulk density, $kg/m^3$
$\Lambda_{zL}$	= axial thermal conductivity, $W/m/K$
$\Delta H_R$	= heat of reaction, $J/mol$

### *Subscripts and Abbreviations*

$G$	= gas
$L$	= liquid
$L_p$	= liquid in the porous volume

<i>m</i>	= model ( $m\varepsilon_L$ = model for the liquid holdup)
M	= Marlotherm (cooling oil)
S	= solid catalyst
St	= stainless steel
W1	= wall 1
W2	= wall 2

## REFERENCES

- Feick, J. and Quon, D. (1970) Mathematical models for the transient behavior of a packed bed reactors. *Can. J. Chem. Eng.* **48**, 205-211.
- Gianetto, A. and Specchia, V. (1992) Trickle-bed reactor: state of art and perspectives. *Chem. Eng. Sci.* **47** (13-14), 3197-3213.
- Herskowitz, M. and Smith, J. M. (1983) Trickle-bed reactors: a review. *A.I.Ch.E. J.* **29** (1), 1-18.
- Hindmarsh A.C. (1980) ACM SIGMUN Newsletter 15.
- Le Lann J.M. (1996) Internal Report, User Manual.
- Specchia, V., Baldi, G. and Gianetto, A. (1978) Solid-liquid mass transfer in concurrent two-phase flow through packed beds. *Ind. Eng. Chem. Process. Des. Dev.* **17** (3), 362-367.
- Stüber, F (1995) Sélectivité en réacteur catalytique triphasique : analyse expérimentale et théorique d'hydrogénations consécutives en lit fixe catalytique à co-courant ascendant de gaz et de liquide. *Ph. D. thesis*. Institut National Polytechnique de Toulouse, ENSIGC, France.
- Stüber, F., Wilhelm, A. M. and Delmas, H. (1996) Modelling of three phase catalytic upflow reactor: a significant chemical determination of liquid-solid and gaz-liquid mass transfer coefficients. *Chem. Eng. Sci.* **51** (10), 2161-2167.
- Syaiful (1992) Réacteurs polyphasiques à cocourant ascendant: influence de la viscosité sur les rétentions, dispersions axiales et transfert gaz-liquide. *Ph. D. thesis*. Institut National Polytechnique de Toulouse, ENSIGC, France.
- Turpin, J.L. and Huntington, R.L. (1967) Prediction of pressure drop for two-phase, two-component concurrent flow in packed beds. *A.I.Ch.E. J.* **13** (6), 1196-1202.
- Visser, J. B. M., Stankiewicz, A., Van Dierendonck, L. L., Manna, L., Sicardi, S. and Baldi, G. (1994) Dynamic operation of a three-phase upflow reactor for the hydrogenation of phenylacetylene. *Catalysis Today* **20**, 485-500.
- Wärna, J. and Salmi, T. (1996) Dynamic modelling of catalytic three phase reactors. *Comput. Chem. Eng.* **20** (1), 39-47.
- Zhukova, T. B., Pisarenko, V. N. and Kafarov, V. V. (1990) Modeling and design of industrial reactors with a stationary bed of catalyst and two-phase gas-liquid flow - a review. *Int. Chem. Eng.* **30** (1), 57-102.

List of captions:

Fig. 1. Simplified drawing of the experimental apparatus.

Fig. 2. Schematic drawing of the heat exchanges through the walls of the reactor.

Fig. 3. Transient concentration profiles at  $t = 10$  mn -  $Q_L = 1.05$  l/h,  $Q_{H2} = 240$  NI/h,  $P = 0.4$  MPa.

Fig. 4. Transient concentration profiles at  $t = 20$  mn -  $Q_L = 1.05$  l/h,  $Q_{H2} = 240$  NI/h,  $P = 0.4$  MPa.

Fig. 5. Steady state concentration profiles -  $Q_L = 1.05$  l/h,  $Q_{H2} = 240$  NI/h,  $P = 0.4$  MPa.

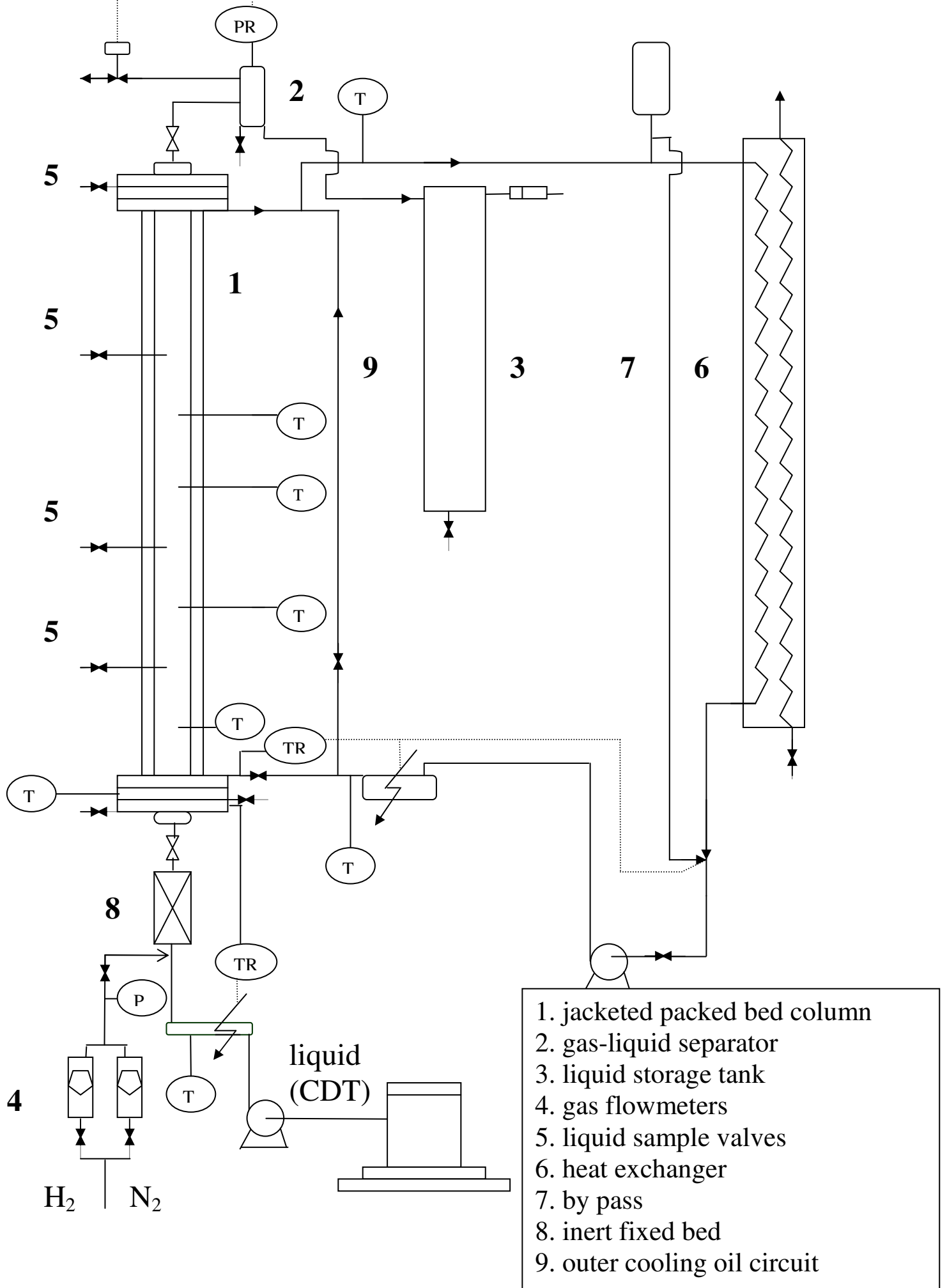
Fig. 6. Start-up: concentration evolution at  $Z = 1.065$  m -  $Q_L = 1$  l/h,  $Q_{H2} = 310$  NI/h,  $P = 0.4$  MPa.

Fig. 7. Start-up: temperature evolution at  $Z = 0.915$  m -  $Q_L = 1$  l/h,  $Q_{H2} = 310$  NI/h,  $P = 0.4$  MPa.

Fig. 8. Concentration evolution at  $Z = 1.065$  m when increasing  $Q_L$  from 0.95 to 1.8 l/h at  $t = 100$  mn -  $Q_{H2} = 350$  NI/h,  $P = 0.4$  MPa.

Fig. 9. Temperature evolution at  $Z = 0.465$  m when increasing  $Q_{H2}$  from 795 to 990 NI/h at  $t = 100$  mn and up to 1350 NI/h at  $t = 105$  mn -  $Q_L = 1.85$  l/h,  $P = 0.4$  MPa.

Figure 1



- 1. jacketed packed bed column
- 2. gas-liquid separator
- 3. liquid storage tank
- 4. gas flowmeters
- 5. liquid sample valves
- 6. heat exchanger
- 7. by pass
- 8. inert fixed bed
- 9. outer cooling oil circuit

Figure 2

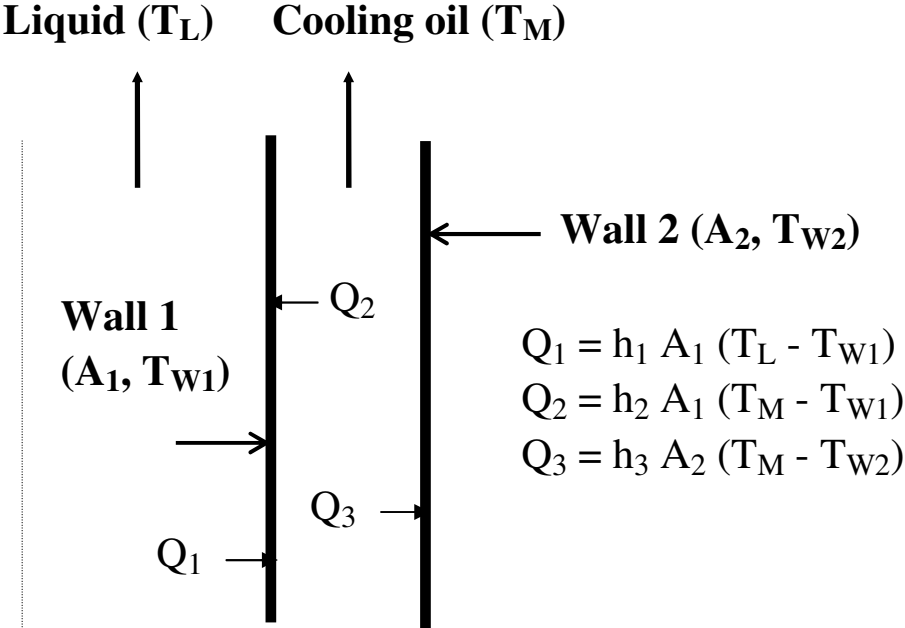


Figure 3

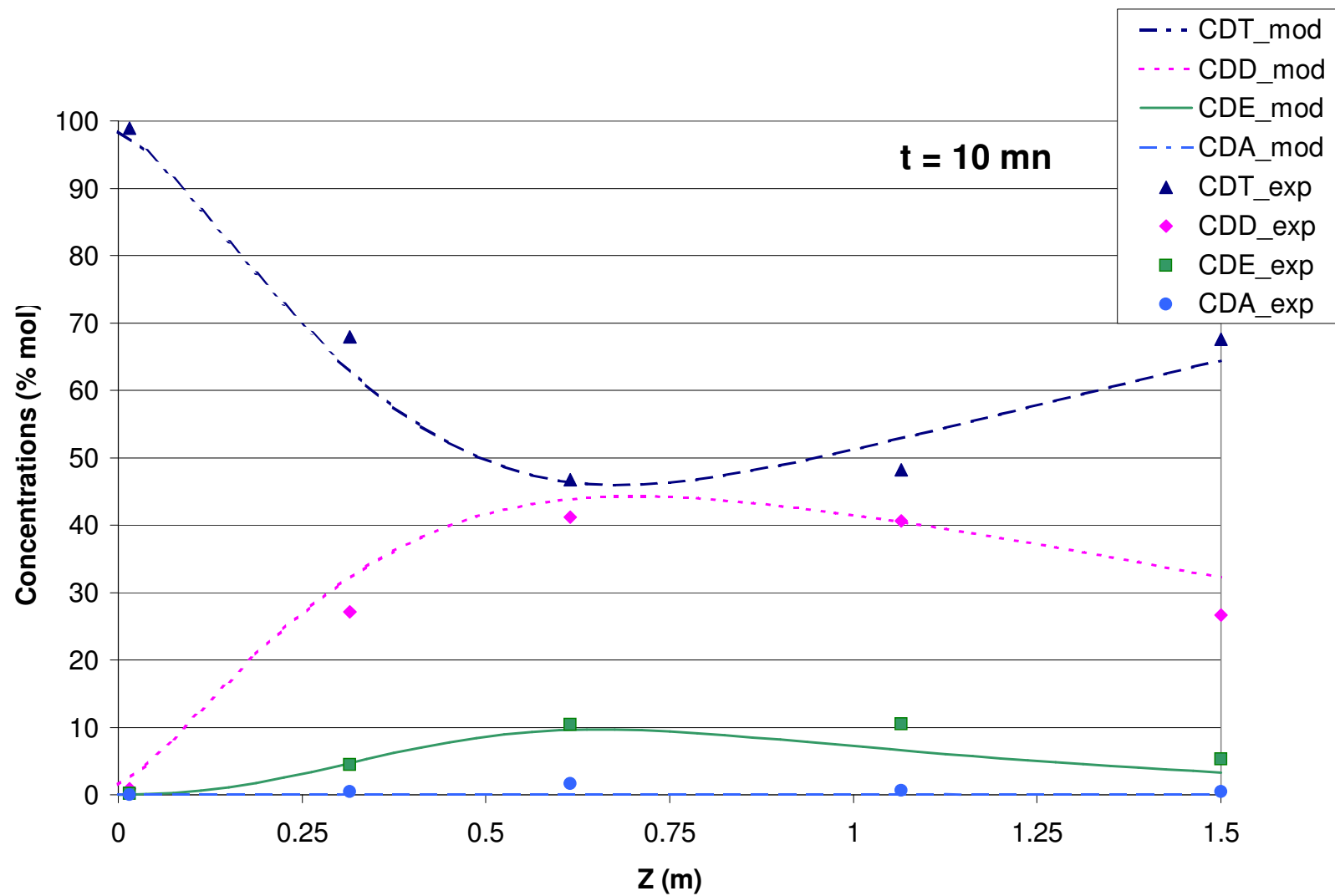


Figure 4

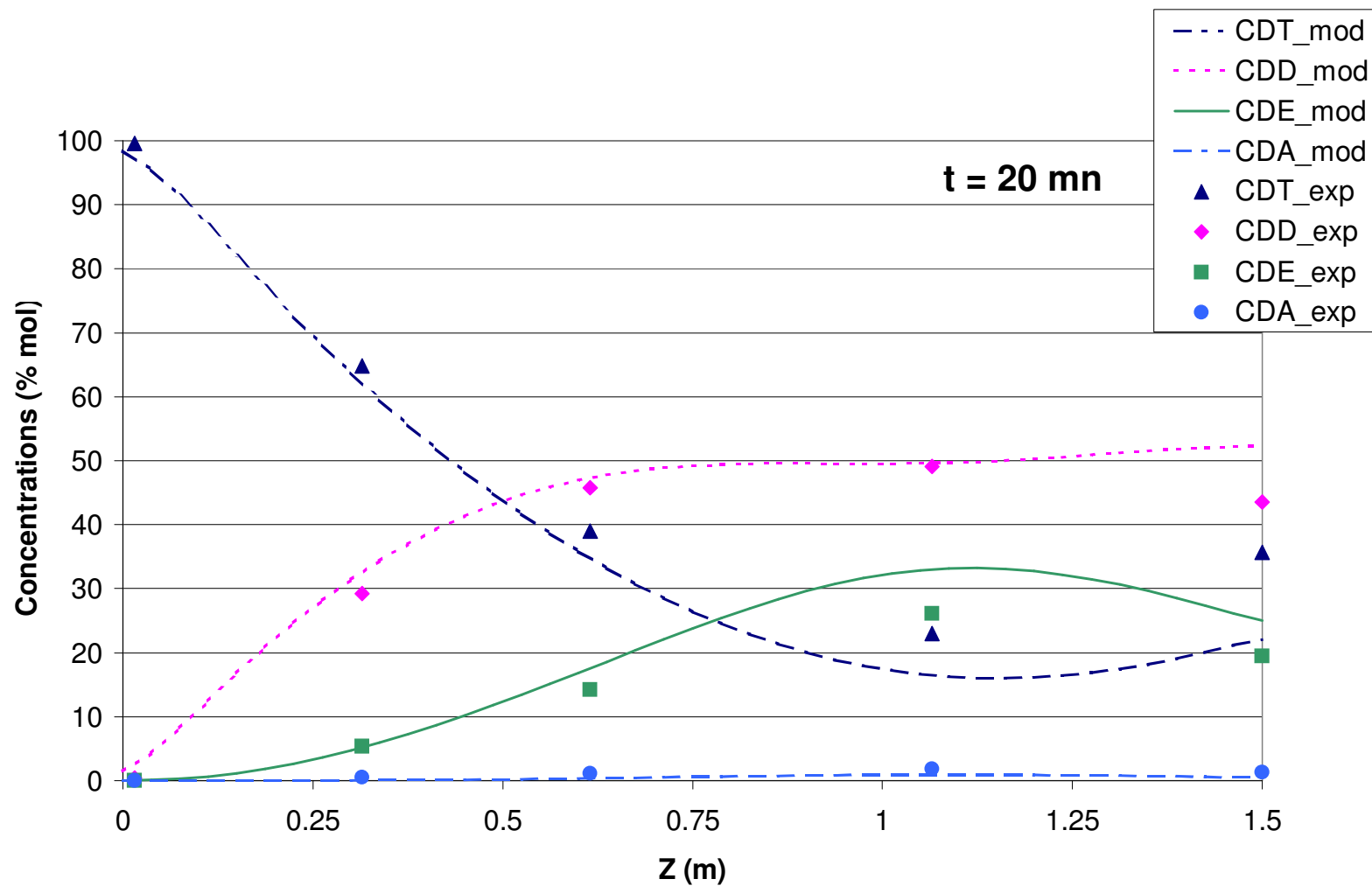


Figure 5

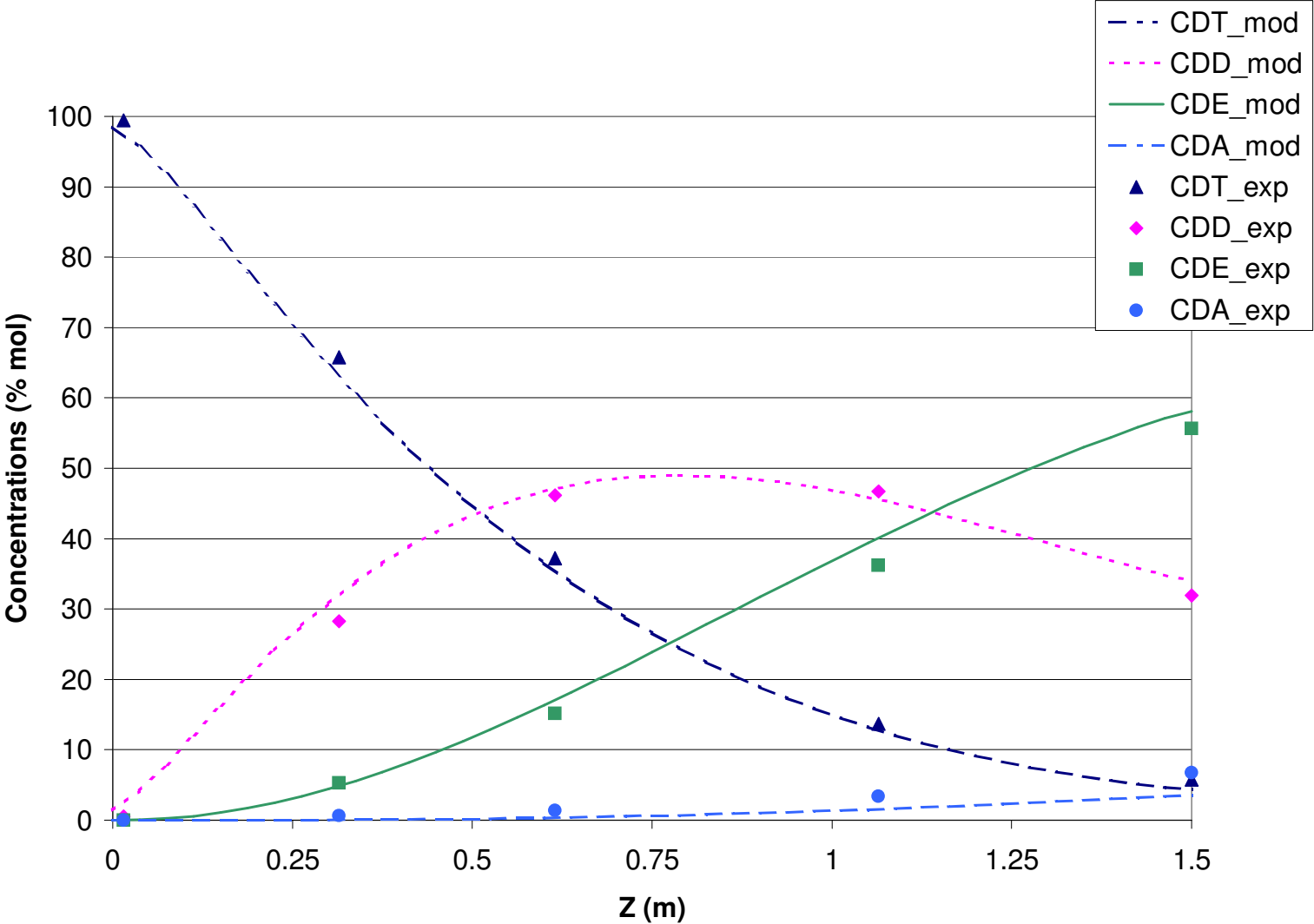


Figure 6

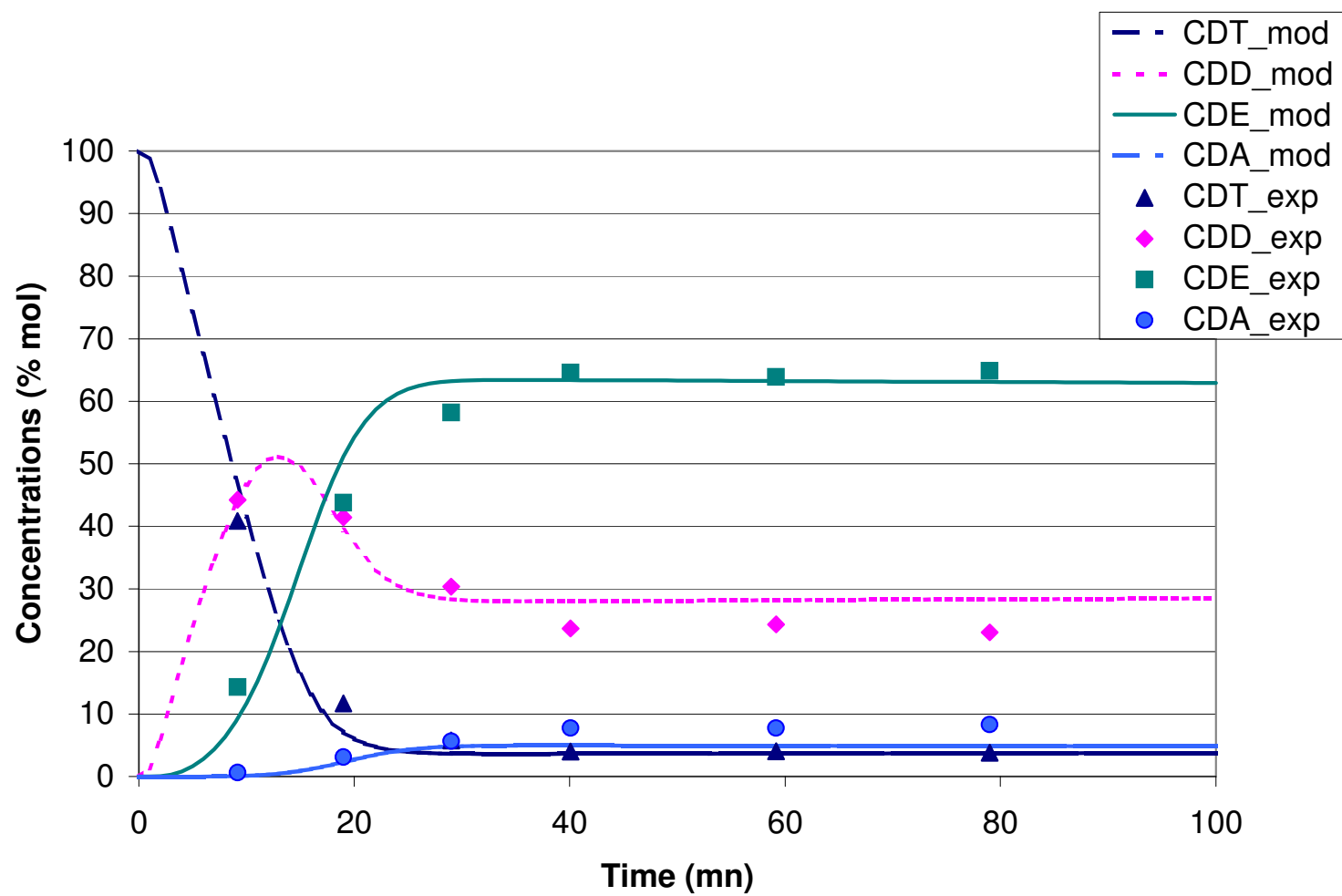


Figure 7

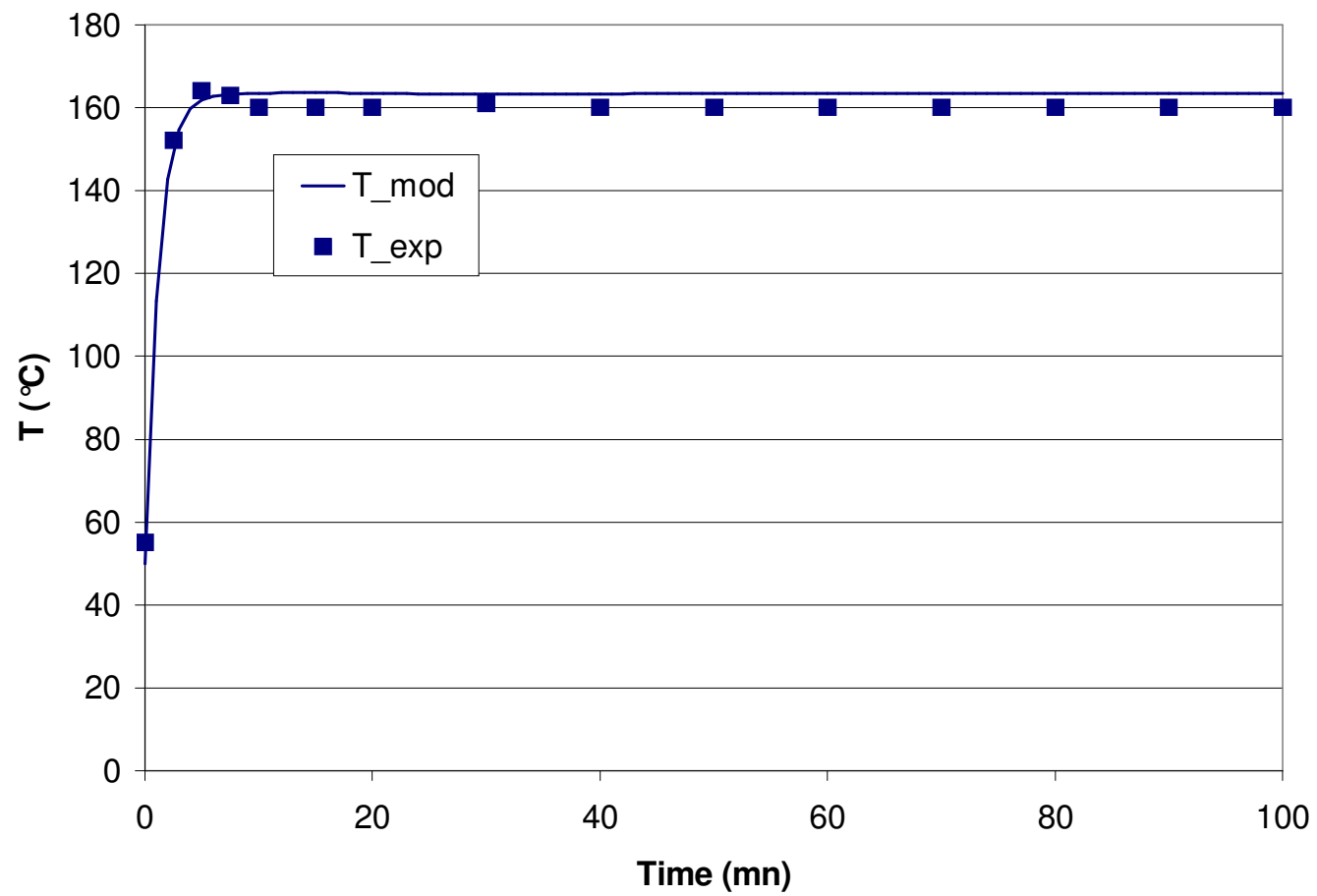


Figure 8

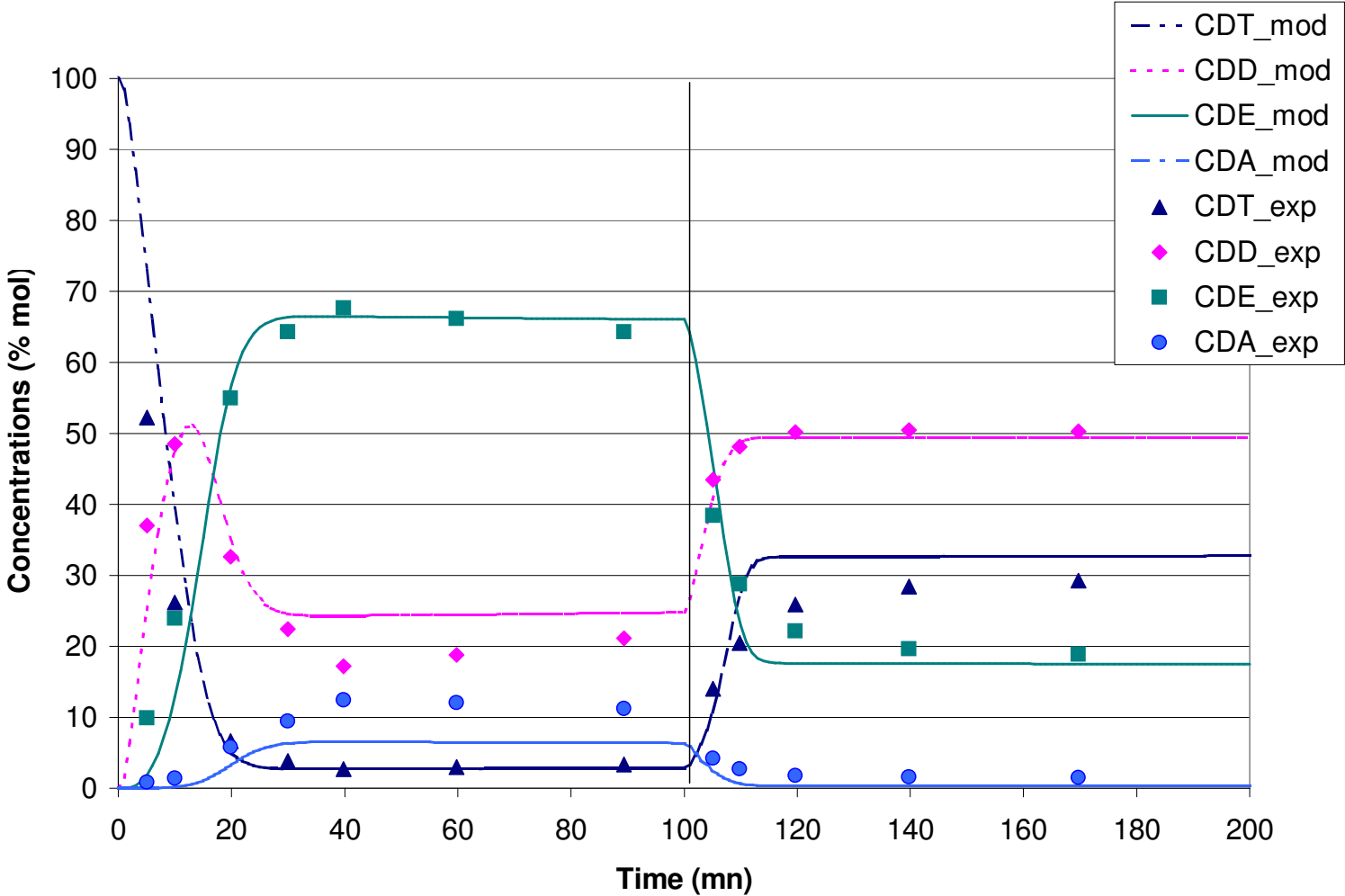


Figure 9

